Amorphous-to-Crystalline Phase Transformation of Thin Film Rubrene

Se-Woong Park, Jeong-Min Choi, Kwang Hyun Lee, Han Woong Yeom, and Seongil Im*

Institute of Physics and Applied Physics, Yonsei University, Seoul 120-749, Korea

Young Kook Lee

Department of Metallurgical Engineering, Yonsei University, Seoul 120-749, Korea

Received: November 2, 2009; Revised Manuscript Received: February 18, 2010

We report on the amorphous-to-crystalline phase transformation of rubrene thin films. The crystallization of the organic thin films displays disk-like domains whose nucleation and growth follow phase transformation kinetics well-established for inorganic materials under certain time and temperature conditions. We understood that the crystallization of amorphous rubrene thin film shows site-saturated nucleation behavior while the crystalline growth involves both diffusion and interface-controlled kinetics displaying spherulitic disk growth behavior. The activation energy of the transformation kinetics was about 0.78 eV on hexamethyldisilazane-functionalized SiO_2 substrate as mostly consumed at the growth process. The crystallization kinetics changes with the film substrate; more hydrophobic substrate induces a lesser number of crystalline nuclei while causing faster growth of those nuclei.

Introduction

Semiconducting organic thin films have attracted much attention during the last and present decades due mainly to the novel applications as active channel of thin film transistors (TFTs).[1−4] For these organic thin film transistors, the most crucial technical issue is to achieve a high carrier mobility of the organic channels. In this respect, the highest mobility organic TFT of rubrene (up to 20 $cm^2/(V\ s)$) is notable.[5−11] However, since such high mobility is only achieved from a single bulk crystal of rubrene which is not a practically applicable form, it is currently very challenging to grow high crystalline quality thin films of rubrene and other organic materials.[12−19] While there has been progress in growing higher quality crystalline thin films of rubrene by solution or vapor processes, the fundamental physical mechanism of the crystallization of the organic thin films has rarely been investigated in detail and is thus only poorly understood. We focus on the physical vapor phase thin film growth, for which two effective crystallization methods of the very-slow-rate growth and the thermal-anneal-induced amorphous-to-crystalline phase transformation were reported.[20,21] In particular, we systematically investigated the amorphous-to-crystalline transformation process of rubrene thin films, that is, by way of annealing the thermally evaporated amorphous films. Indeed, only a few studies exist so far for the crystallization of small-molecule-composed amorphous thin films, while the crystallization of polymer chains has been extensively studied.[22−28] The nucleation and growth of disk-shaped crystalline domains within the amorphous rubrene thin films were observed and compared with a spherulitic nucleation/growth behavior,[29,30] and their growth rates were characterized in detail as a function of temperature. We demonstrate that this crystallization process could be quantitatively analyzed by the classical nucleation and growth kinetics established for the inorganic bulk materials.[31,32] For the given conditions of the substrates (the functionalized or bare SiO_2) and of the postanneal temperature range (50−80 °C), the crystallization process is nucleation-site-saturated with both the diffusion- and interface-controlled behavior showing an overall kinetic barrier of 0.78 eV. We thus suggest that such classical phase transformation theories might be widely applicable to developing a novel growth method of high quality organic crystalline films, playing as a gateway to the microscopic understanding of the involved physical processes.

Experimental Methods

Our rubrene thin films were deposited mainly on hexamethyldisilazane (HMDS)-functionalized but also on 7-octenyltrichlorosilane (7-OTS)-functionalized and bare SiO_2 substrates as well. It is well-known that the surface of HMDS-functionalized SiO_2 is moderately hydrophobic (deionized water contact angle, $\theta = 60°$) and 7-OTS-functionalized SiO_2 is very much hydrophobic ($\theta = 80°$) while that of bare SiO_2 is quite hydrophilic ($\theta = 40°$) with a large surface energy. On these prepared samples, rubrene thin films were deposited with a deposition rate of 0.1 nm/s by thermal evaporation in a vacuum chamber with a base pressure of 1×10^{-6} Torr at a substrate temperature of 40 °C. The film thickness was about 80 nm, as monitored by quartz oscillation and confirmed by ellipsometry. After deposition, we carried out in situ postannealing at various substrate temperatures of 50, 60, 70, and 80 °C for various periods, to observe the temperature- and time-dependent evolution of crystalline domains. After annealing, the crystalline and amorphous morphology in the films were characterized by optical microscopy and atomic force microscopy (AFM). X-ray diffraction was conducted for crystallized rubrene films with 80 and 200 nm thicknesses, using a Cu Kα target.

Results and Discussion

Figure 1 shows the optical microscope images of a rubrene thin film surface prepared on HMDS-functionalized SiO_2 by in situ annealing following the thermal deposition at 40 °C. The rubrene films shown in Figure 1a−c were annealed at 70 °C

* Corresponding author. E-mail: semicon@yonsei.ac.kr. Phone: 82-2-2123-2842. Fax: 82-2-392-1592.

10.1021/jp910459p
Published on Web 04/14/2010

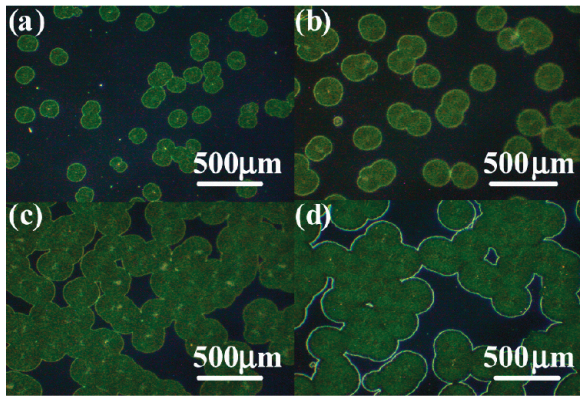

Figure 1. Optical microscope images of rubrene thin film surfaces. The film was deposited on HMDS at 40 °C and then in situ annealed at 70 °C for (a) 3 h, (b) 5 h, and (c) 8 h. Figure 1d shows the result from in situ annealing at 80 °C for 4 h.

for 3, 5, and 8 h, while Figure 1d shows the film surface obtained after annealing at 80 °C for 4 h. The amorphous phase film initially has no extra domains but begins to have disk-shaped domains which grow in diameter as time elapses. Figure 1a shows many discs which have ~130 μm as an average diameter of rubrene crystals, while the size increases up to 290 μm after a few hours (Figure 1c). The disk area coverage (or volume fraction) also increases from 17% of Figure 1a to 76% of Figure 1c. Comparing the two samples of Figure 1c and d, we simply find that postanneal at a higher temperature leads to a faster disk growth than at a lower temperature.

Morphological property differences between the disk and amorphous rubrene have been displayed in the AFM image of Figure 2a, where the two phases in a 70 °C-annealed rubrene film were clearly distinguished as the film surface was scanned. The disk domain region displayed directional-lamellae structures with the surface of a large rms roughness (~10 nm), while the amorphous region showed a flat and smooth surface with a rms roughness of less than 2 nm. For more details, we can observe that the disk region of the thin film is higher than the amorphous region in height (by ~20 nm as measured with AFM) and there exists an interesting narrow trench at the phase boundary between the two regions, where the trench depth was ~60 nm which is comparable to the initial amorphous thickness (80 nm). According to this phase boundary contour, it is reasoned that this directional disk growth involves consumption of amorphous rubrene at the interface (interface reaction involving molecule attachment) and also involves the mass-transport (diffusion) from the amorphous background, implying the mixed-controlled growth behavior.

The directional growth of discs is considered as spherulitic growth behavior, which is often found in polymer film growth.[33−36] As illustrated in the inset of Figure 2b, the spherulite disk nucleates from a primary point and grows radially with directional lamellae or fibers. These fibers proceed in a direction, but due to some thermodynamic instabilities, new crystalline fibers branch into the other directions, maintaining a disk shape as a whole.[37−39] Interestingly, this type of spherulitic growth has not been reported in small-molecule-composed organic thin film except the present work. According to the XRD spectra of Figure 2b, only the (200) crystalline orientation of the films is clearly observed from the sphrulitic rubrene crystal films that should have an orthorhombic structure. Here, we annealed the as-deposited rubrene films at 80 °C for 24 h in a vacuum, to guarantee the perfect crystallization of the amorphous rubrene, and the (200) peak appeared more intense with

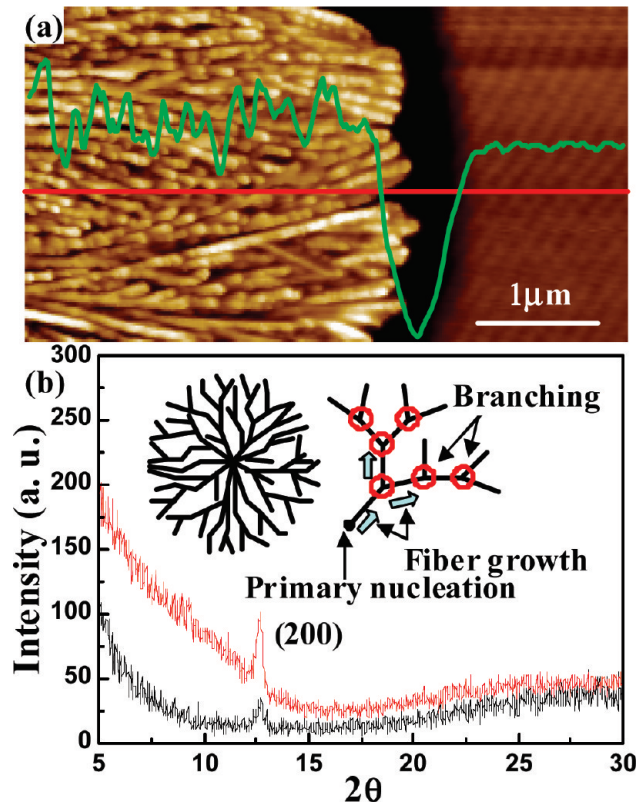

Figure 2. (a) 5 × 5 μm^2 AFM surface image of the border area containing the amorphous matrix and the crystalline disk. The green line is one-dimensional roughness contour obtained by scanning the surface along the red line. (b) X-ray diffraction spectra of two rubrene thin films totally covered by the sphrulitic crystalline discs; the spectra show the (200) preferred orientation of 200 and 80 nm thick rubrene films that were annealed at 80 °C for 24 h in a vacuum.

200 nm thick film than with 80 nm thin film. This *a*-axis preferred orientation may also be worthwhile to note because usual small molecule crystalline films including pentacene and tetracene have shown *c*-axis preferred orientation on any substrates as directly crystallized by vacuum deposition.

The physical property differences between amorphous and crystalline thin film rubrene were also measured. As photoluminescence (PL) spectra were achieved with three rubrene films annealed at 70 °C for 0, 3, and 8 h, totally amorphized rubrene film displays the highest peak intensity at 560−580 nm, while mostly disk-covered rubrene has a much reduced intensity (Figure 3a). It is well-known that strong PL emission originates from the amorphous phase in organics, but the intensity becomes much reduced with the increase of crystalline ordering.[40] In contrast to the PL behavior, direct absorption characteristics, as measured with the same rubrene thin films, display the increase of crystalline rubrene signal[41] intensity with the increase of disk coverage in Figure 3b.

Figure 4a shows the plots of annealing time (t) vs average radius (r) of crystalline rubrene discs as obtained from different annealing temperatures at 50, 60, 70, and 80 °C. From these plots, we could extract out the crystalline growth rate and growth mechanism as well, based on the general growth equation, $r \sim t^m$.[31,32,42,43] The growth parameter, m, is between 0.5 and 1, and can be calculated from the slope of the plots of Figure 4a. The growth mechanism is generally divided into two categories: diffusion-controlled growth with $m = 0.5$ and interface (reaction)-controlled growth with $m = 1$. In the present study, the measured m values are 0.66, 0.77, and 0.77 for 50, 60, and 70 °C, respectively. It means that the crystalline growth of rubrene

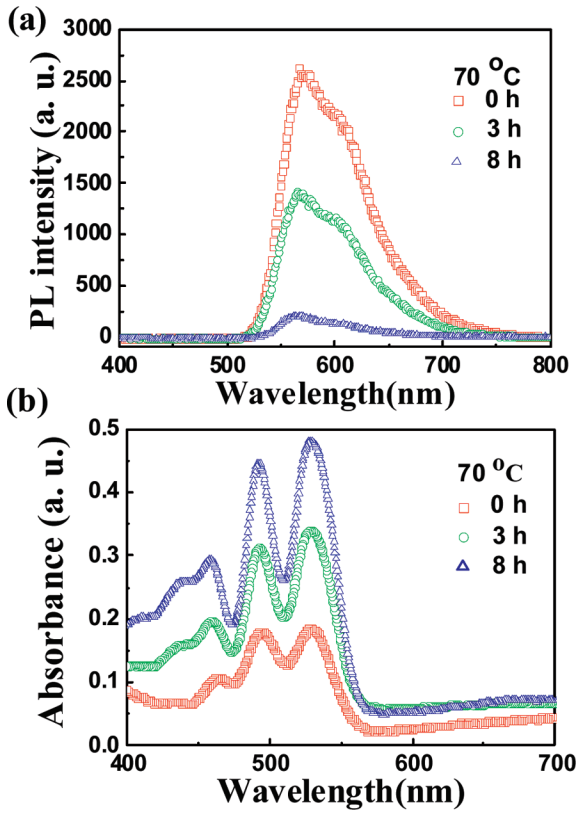

Figure 3. (a) Photoluminescence (PL) spectra and (b) optical absorption spectra of rubrene thin film as annealed at 70 °C for 0, 3, and 8 h.

thin film possesses a mixed manner of diffusion and interface control, as we already predicted from the amorphous/crystalline interface contour of Figure 2a. Figure 4b shows the plots of annealing time (t) vs crystalline rubrene volume fraction (x) as obtained from the thin films postannealed at various substrate temperatures of 50, 60, 70, and 80 °C. From the plots, Avrami parameters were estimated to further understand the amorphous-to-crystallization phase transformation mechanism in a more detailed manner, particularly including the nucleation behavior of crystalline discs. The parameters can be obtained from the well-known JMA (Johnson−Mehl−Avrami) equation which was developed to estimate general phase transformation kinetics[31,32]

$$x = 1 - \exp(-bt^n) \quad (1)$$

where x is the volume fraction of crystalline discs, b is the prefactor that is actually the function of temperature containing the transformation activation energy (Q_a) term, and n is the Avrami exponent. According to Figure 4a, the n values of 50, 60, and 70 °C annealed samples are 1.51, 2.06, and 2.20, respectively. These n values are in the range $1.50 \leq n < 2.50$, which indicates that the amorphous-to-crystallization process follows "site-saturated nucleation" behavior.[31,44,45] That is to say, in the current type of phase transformation, a constant number of nucleation sites is initially occupied and then only growth continues without any further nucleation events during the whole process. As a matter of fact, the optical microscopy results in Figure 1 display that the discs observed in a certain annealing time and temperature frame seem to have almost an identical diameter, and more surprisingly that almost the same number of discs was kept regardless of annealing time and temperature.

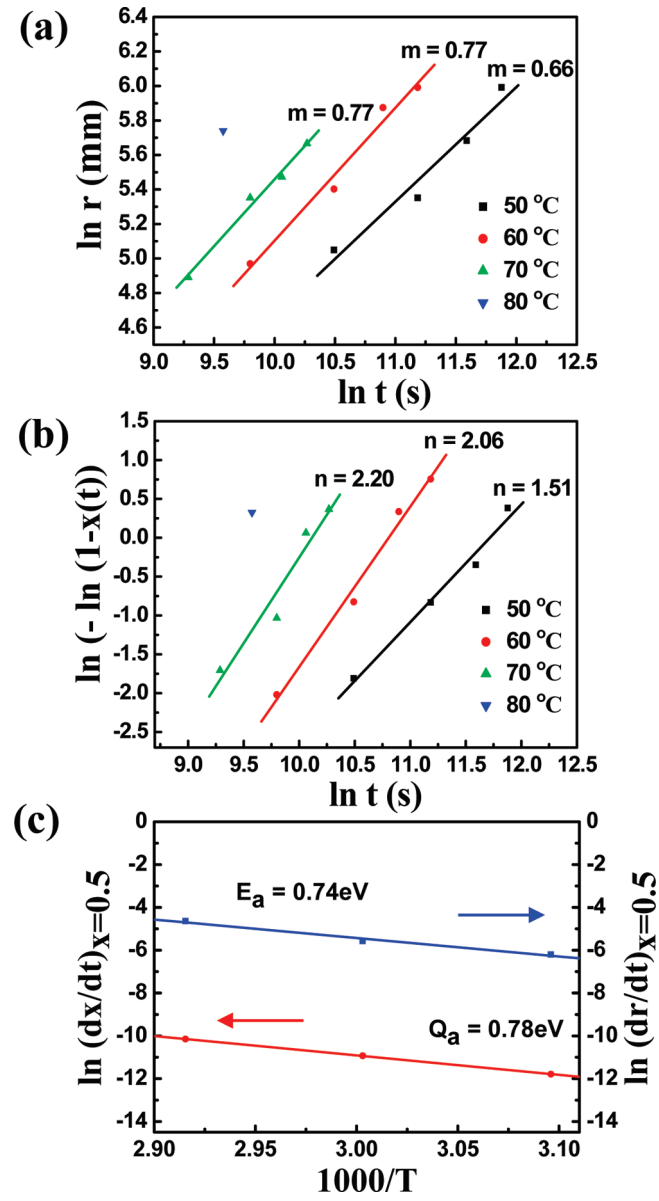

Figure 4. (a) Plots of rubrene disk radii vs annealing time as obtained at 50, 60, 70, and 80 °C. (b) Avrami plot of annealing time vs disk volume fraction as obtained at given temperatures. (c) Transformation rate and growth rate (Arrhenius) plots to estimate the respective activation energies; Q_a was 0.78 eV, and E_a was 0.74 eV.

The nucleation sites can be any mechanical dent or rough points and any defects on the surface of HMDS-functionalized substrate, and it is likely that the number density of those nucleation probable sites would be fixed by the topographical and chemical conditions of a substrate prior to rubrene deposition and postanneal. In the present study, the prefactor, b, was also extracted out for each anneal temperature from the plot of Figure 4b, to achieve a perfect Avrami equation. Then, by combining eq 1 and the following equation (eq 2) which originates from "the change of slope" technique,[46] we could work out an activation energy (Q_a) for the amorphous-to-crystalline phase transformation:

$$\ln(dx/dt)_{x,T} = \text{constant} - Q_a/kT \quad (2)$$

where k is the Boltzmann constant and T is the temperature in kelvin. The down-side plot in Figure 4c shows the plot to

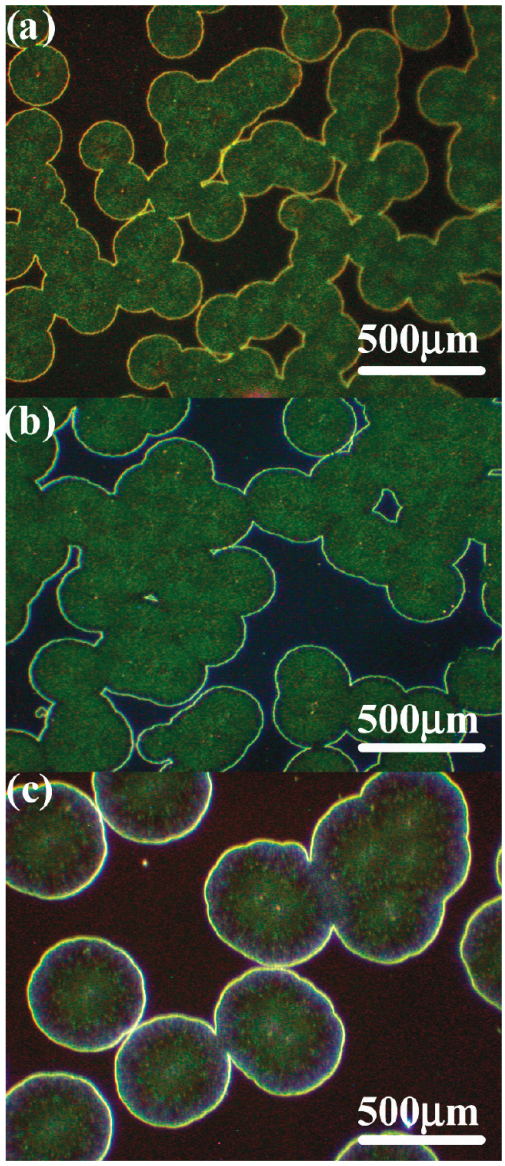

Figure 5. Influence of the substrate on the rubrene thin film crystallization. Optical microscope images show the disk growth behavior on (a) SiO_2, (b) HMDS, and (c) 7-OTS in the order of hydrophobicity as the rubrene films were deposited at 40 °C and followed the postanneal at 80 °C for 4 h.

achieve an activation energy for amorphous-to-crystalline phase transformation as obtained under the condition at $x = 0.5$. From this plot, we achieved a Q_a value of 0.78 eV. (Similarly, we achieved Q_a values of 0.70 and 0.90 eV at $x = 0.2$ and 0.8.) This value is comparable to ~1 eV which is for the crystallization of various polymers.[47−49] Hence, it seems that the crystallization of amorphous rubrene film (composed of rubrene monomers) is somewhat easier than that of amorphous polymer films. On the other hand, we can simply obtain another plot which explains only the growth rate of crystalline discs at the time of $x = 0.5$, as shown in the upper plot. The relationship between the growth rate (dr/dt) and the activation energy (E) of crystal growth obeys Arrhenius law, $dr/dt = r_o \exp(-E_a/kT)$, where E_a is the activation energy barrier for the growth of crystalline rubrene. Since we obtained 0.74 eV as E_a which is very close but a little lower than Q_a, 0.78 eV, we regard that the activation energy for the phase transformation is mostly for the growth of crystalline discs rather than for their nucleation.

Figure 5a, b, and c shows three respective optical microscope images of rubrene thin film surface prepared on bare, HMDS-functionalized, and 7 OTS-functionalized SiO_2 substrates, which went through the same in situ annealing at 80 °C for 4 h. We performed these experiments to see how the substrate affects the nucleation and growth of the rubrene discs. Similar disk-shaped domains were obtained on the bare SiO_2, but unlike the case on the HMDS-functionalized SiO_2, the discs of smaller diameter and higher number density were observed on the bare SiO_2, revealing that both the nucleation and growth behaviors are significantly influenced by the surface state of the substrate. Interestingly, the 7-OTS-functionalized case was quite opposite to that of the bare SiO_2 case, displaying an obviously larger diameter and lower number density of discs. It is no wonder if the size of discs is somewhat proportional to the hydrophobicity of substrate, since a more hydrophobic surface will provide less interfacial energy for the hydrophobic rubrene disk, reducing the activation barrier for the growth. A little mysterious is why more hydrophobic substrate results in a lesser number of discs. We cannot show any supporting experimental evidence here but can provide a conjecture that the hydroxyl OH groups initially present on the surface may act as the nucleation sites for the crystalline rubrene.[50]

Conclusions

In summary, the present work indicates that the crystallization of the amorphous rubrene thin films displays spherulitic disk-like domains whose nucleation and growth can be understood on the basis of the well-established JMA theory. The amorphous-to-crystalline phase transformation of rubrene thin film shows site-saturated nucleation behavior, and the crystalline growth involves both diffusion- and interface-controlled processes. The activation energy of the transformation kinetics was about 0.78 eV, mostly consumed at the growth process, and this transformation is facilitated on more strongly hydrophobic substrate of lower surface energy. This fundamental study is possibly exploited to develop a novel growth method for a wide variety of high quality organic crystalline thin film materials.

Acknowledgment. The authors acknowledge financial support from KOSEF (NRL program: Grant No. 2009-8-0403), Brain Korea 21 Project and MKE (21st century Frontier R&D Program: No. F0004022-2008-31). Among these authors, S.-W.P. acknowledges the support from the National Graduate Science and Technology Scholarship, Republic of Korea. Seongil Im and YK Lee give sincere thanks to the lifelong devotion of Prof. CS Choi on phase transformation theory.

References and Notes

(1) Eder, F.; Klauk, H.; Halik, M.; Zschieschang, U.; Schumid, G.; Dehm, C. *Appl. Phys. Lett.* **2004**, *84*, 2673.
(2) Bao, Z. *Adv. Mater.* **2000**, *12*, 227.
(3) Li, L.; Tang, Q.; Li, H.; Hu, W. *J. Phys. Chem. B* **2008**, *112*, 10405.
(4) Schmit, R.; Oh, J. H.; Sun, Y.; Deppisch, M.; Krause, A.; Radacki, K.; Braunschweig, H.; Könemann, M.; Erk, P.; Bao, Z.; Würthner, F. *J. Am. Chem. Soc.* **2009**, *131*, 6215.
(5) Sundar, V. C.; Zaumseil, J.; Podzorv, V.; Menard, E.; Willett, R. L.; Someya, T.; Gerhenson, M. E.; Rogers, J. A. *Science* **2004**, *303*, 1644.
(6) Menard, E.; Podzorov, V.; Hur, S.; Gaur, A.; Gershenson, M. E.; J. A.; Rogers, J. A. *Adv. Mater.* **2004**, *16*, 2097.
(7) Hulea, I. N.; Fratini, S.; Xie, H.; Mulder, C. L.; Iossad, N. N.; Rastelli, G.; Cluchi, S.; Morpurgo, A. F. *Nat. Mater.* **2006**, *5*, 982.
(8) Zeis, R.; Besnard, C.; Siegrist, T.; Schlockermann, C.; Chi, X.; Kloc, C. *Chem. Mater.* **2006**, *18*, 244.
(9) Wen, S.; Li, A.; Song, J.; Deng, W.; Deng, K.; Han, K.; Goddard, W., III. *J. Phys. Chem. B* **2009**, *113*, 8813.
(10) Butko, V. Y.; Lashley, J. C.; Ramirez, A. P. *Phys. Rev. B* **2005**, *72*, 081312.

(11) Takeya, J.; Nishikawa, T.; Takenobu, T.; Iwasa, Y.; Mitani, T.; Goldmann, C.; Krellner, C.; Batlogg, B. *Appl. Phys. Lett.* **2004**, *85*, 5078.
(12) Käfer, D.; Witte, G. *Phys. Chem. Chem. Phys.* **2005**, *7*, 2850.
(13) Seo, S.; Park, B.; Evans, P. G. *Appl. Phys. Lett.* **2006**, *88*, 232114.
(14) Stingelin-Stutzmann, N.; Smits, E.; Wondergem, H.; Tanase, C.; Blom, P.; Smith, P.; Deleeuw, D. *Nat. Mater.* **2005**, *4*, 601.
(15) Ishii, Y.; Shimada, T.; Okazaki, N.; Hasegawa, T. *Langmuir* **2007**, *23*, 6864.
(16) Seo, J.; Pedersen, T.; Chang, G.; Moewes, A.; Yoo, K.; Cho, S.; Whang, C. *J. Phys. Chem. B* **2007**, *111*, 9513.
(17) Zeng, X.; Wang, L.; Duan, L.; Qiu, Y. *Cryst. Growth Des.* **2008**, *8*, 1617.
(18) Campione, M. *J. Phys. Chem. C* **2008**, *112*, 16178.
(19) Pivetta, M.; Blüm, M.; Pattthey, F.; Schneider, W. *J. Phys. Chem. B* **2009**, *113*, 4578.
(20) Hsu, C. H.; Deng, J.; Staddon, C. R.; Beton, P. H. *Appl. Phys. Lett.* **2007**, *91*, 193505.
(21) Park, S. -W.; Jeong, S. H.; Choi, J. -M.; Hwang, J. M.; Kim, J. H.; Im, S. *Appl. Phys. Lett.* **2007**, *91*, 033506.
(22) Loo, Y.; Register, R. A.; Ryan, A. J. *Phys. Rev. Lett.* **2000**, *84*, 4120.
(23) Xu, J. -T.; Fairclough, J. P. A.; Mai, S.; Ryan, A. J.; Chaibundit, C. *Macromolecules* **2002**, *35*, 6937.
(24) Xiao, J.; Zhang, H.; Wan, X.; Zhang, D.; Zhou, Q. -F.; Woo, E. M.; Turner, S. R. *Polymer* **2002**, *43*, 3683.
(25) Shafee, E. E.; Ueda, W. *Eur. Polym. J.* **2001**, *38*, 1327.
(26) Lorenzo, M. L. D. *Polymer* **2001**, *42*, 9441.
(27) Qiu, Z.; Yan, C.; Yang, W.; Ikehara, T.; Nishi, T. *J. Phys. Chem. B* **2007**, *111*, 2783.
(28) Johcheray, T.; Denoncourt, K.; Meier, M.; Schubert, U.; Duran, R. *Langmuir* **2007**, *23*, 2423.
(29) Luo, Y.; Burn, M.; Rannou, P.; Grevin, B. *Phys. Status Solidi* **2007**, *204*, 1851.
(30) Djuric, T.; Thierry, A.; Grogger, W.; Al-Baqi, S.; Sitter, H.; Resel, R. *Physica E* **2009**, *41*, 1718.
(31) Christian, J. W. *The Theory of Transformation in Metals and Alloys*, 2nd ed.; Pergamon Press: Oxford, U.K., 1975.
(32) Porter, D. A.; Easterling, K. E. *Phase Transformations in Metals and Alloys*; Van Nostrand Reinhold: New York, 1981.
(33) Xu, J.; Guo, B.; Zhou, J.; Li, L.; Wu, J.; Kowalczuk, M. *Polymer* **2005**, *46*, 9176.
(34) Ikehara, T.; Kimura, H.; Qiu, Z. *Macromolecules* **2005**, *38*, 5104.
(35) Lee, J.; Choi, M.; Im, J.; Hwang, D.; Lee, K. *Polymer* **2007**, *48*, 2980.
(36) Liang, G.; Xu, J.; Fan, Z. *J. Phys. Chem. B* **2007**, *111*, 11921.
(37) Gránásy, L.; Pusztai, T.; Börzsönyi, T.; Warren, J. *Nat. Mater.* **2004**, *3*, 645.
(38) Gránásy, L.; Puszti, T.; Tegze, G.; Warren, J.; Douglas, J. *Phys. Rev. E* **2005**, *72*, 011605.
(39) Yang, X.; Sawant, P. *Adv. Mater.* **2002**, *14*, 421.
(40) Pope, M.; Swenberg, C. E. *Electronic process in Organic Crystals and Polymers*, 2nd ed.; Oxford University Press: New York, 1999; pp 40−43.
(41) Najafov, H.; Biaggio, I. *Phys. Rev. Lett.* **2006**, *96*, 056604.
(42) Kim, S. J.; Kim, J. E.; Yang, Y. S. *Solid State Commun.* **2002**, *122*, 135.
(43) Kotula, P. G.; Carter, C. B. *Phys. Rev. Lett.* **1996**, *77*, 3367.
(44) Henderson, D. W. *J. Therm. Anal.* **1979**, *15*, 325.
(45) Lothongkum, G.; Ratanamahasakul, S.; Wangyao, P. *Acta Metallurgica Slovaca* **2005**, *11*, 54.
(46) Jena, A. K.; Chaturvedi, M. C. *Phase Transformation in Materials*; Prentice Hall: Englewood Cliffs, NJ, 1992; pp 111−114.
(47) Liu, S. L.; T. S. Chung, T. S. *Polymer* **1999**, *41*, 2781.
(48) Zhu, X.; Li, Y.; Yan, D.; Fang, Y. *Polymer* **2001**, *42*, 9217.
(49) Van der Wielen, M. W. J.; Cohen Stuart, M. A.; Fleer, G. J.; Schlatmann, A. R.; De Boer, D. K. *Phys. Rev. E* **1999**, *60*, 4252.
(50) Choi, J. -M.; Jeong, S. H.; Hwang, D. K.; Im, S.; Lee, B. H.; Sung, M. M. *Org. Electron.* **2009**, *10*, 199.

JP910459P